Valley Zeeman splitting of monolayer MoS_2 probed by low-field magnetic circular dichroism spectroscopy at room temperature

Y. J. Wu,[1,2] C. Shen,[1,2,a)] Q. H. Tan,[1,2] J. Shi,[2,3] X. F. Liu,[3] Z. H. Wu,[4] J. Zhang,[1,2] P. H. Tan,[1,2] and H. Z. Zheng[1,2]

[1]*State Key Laboratory of Superlattices and Microstructures, Institute of Semiconductors, Chinese Academy of Sciences, Beijing 100083, People's Republic of China*
[2]*College of Materials Science and Opto-Electronic Technology, University of Chinese Academy of Sciences, Beijing 100049, People's Republic of China*
[3]*Division of Photonics, CAS Key Laboratory of Standardization and Measurement for Nanotechnology, CAS Center for Excellence in Nanoscience, National Center for Nanoscience and Technology, Beijing 100190, People's Republic of China*
[4]*MEDIT, Institute of Microelectronics, Chinese Academy of Sciences, Beijing 100029, People's Republic of China*

(Received 4 February 2018; accepted 27 March 2018; published online 11 April 2018)

The valley Zeeman splitting of monolayer two-dimensional (2D) materials in the magnetic field plays an important role in the valley and spin manipulations. In general, a high magnetic field (6–65 T) and low temperature (2–30 K) were two key measurement conditions to observe the resolvable valley Zeeman splitting of monolayer 2D materials in current reported experiments. In this study, we experimentally demonstrate an effective measurement scheme by employing magnetic circular dichroism (MCD) spectroscopy, which enables us to distinguish the valley Zeeman splitting under a relatively low magnetic field of 1 T at room temperature. MCD peaks related to both A and B excitonic transitions in monolayer MoS_2 can be clearly observed. Based on the MCD spectra under different magnetic fields (−3 to 3 T), we obtained the valley Zeeman splitting energy and the g-factors of A and B excitons, respectively. Our results show that MCD spectroscopy is a high-sensitive magneto-optical technique to explore the valley and spin manipulation in 2D materials. *Published by AIP Publishing.*
https://doi.org/10.1063/1.5024766

Two-dimensional (2D) layered materials have captured wide attention of scientific community due to their peculiar optical and electronic properties.[1–4] Among them, transition metal dichalcogenides (TMDs) are outstanding for their advantages in optoelectronic and photonic applications.[5–7] Owing to the spatial confinement and reduced dielectric screening, the binding energy of the excitons in monolayer semiconducting TMDs reaches hundreds of meV.[8–10] Hence, the excitonic transitions are dominant even at room temperature.[11] Another attractive feature of monolayer TMDs is the strong coupling of valley and spin magnetic moments. As discussed in the recent literature,[12–15] there are three sources of magnetic moment, which might contribute to the total Zeeman shift: spin magnetic moment, atomic orbital magnetic moment, also labeled as intracellular magnetic moment, and valley orbital magnetic moment that is associated with the Berry curvature, also labeled as intercellular magnetic moment.

Monolayer MoS_2 possesses a direct bandgap that is located at the energy-degenerate yet inequivalent K and K' valleys. Its strong spin-orbit coupling splits the conduction and valence bands into spin-up and spin-down components, respectively. The splitting in the conduction band is small (∼5 meV), while that in the valence band is rather large (∼150 meV), thus giving rise to well-separated A and B excitonic transitions.[16] Moreover, the spin-orbit splittings are of the same magnitude but opposite signs at valleys K and K', leading to a valley-dependent optical selection rule:[14,15,17] light of $\sigma+$ ($\sigma-$) circular polarization exclusively couples to inter-band excitonic transitions in the K (K') valley, as shown in Fig. 1(a). It also depicts the Zeeman shift of the conduction and valence bands in the K and K' valleys under a perpendicular magnetic field. The solid (dashed) curves are the conduction and valence bands at a positive (zero) magnetic field. The spin magnetic moment, atomic orbital magnetic moment, and valley magnetic moment are marked with black, cyan, and green arrows, respectively. When monolayer MoS_2 is placed in a perpendicular magnetic field, its energy bands near K and K' valleys shift oppositely due to the valley Zeeman effect, which is proportional to the magnetic field and effective g-factor. Therefore, the measurement of energy band splitting and the g-factor is meaningful for the study of coupling of different magnetic moments.

Recently, the valley Zeeman effect of different 2D materials which attracted a lot of attention was studied *via* polarization-resolved magneto-optical spectroscopy such as photoluminescence and absorption.[13–15,17–19] The feasibility and reliability of such methods are seriously dependent on the accurate determination of spectral peak positions, and thus, high magnetic fields (6–65 T) and low temperatures (2–30 K) are indispensable. The requirements of such high magnetic fields and low temperatures are great handicaps for the extensive study of monolayer valleytronics.

In this work, we measured the excitonic Zeeman splittings of monolayer MoS_2 with a home-built microscopic magnetic circular dichroism (MCD) system. The experimental principle and measurement setup are shown in Figs. 1(b) and

a)Electronic mail: shenchao@semi.ac.cn

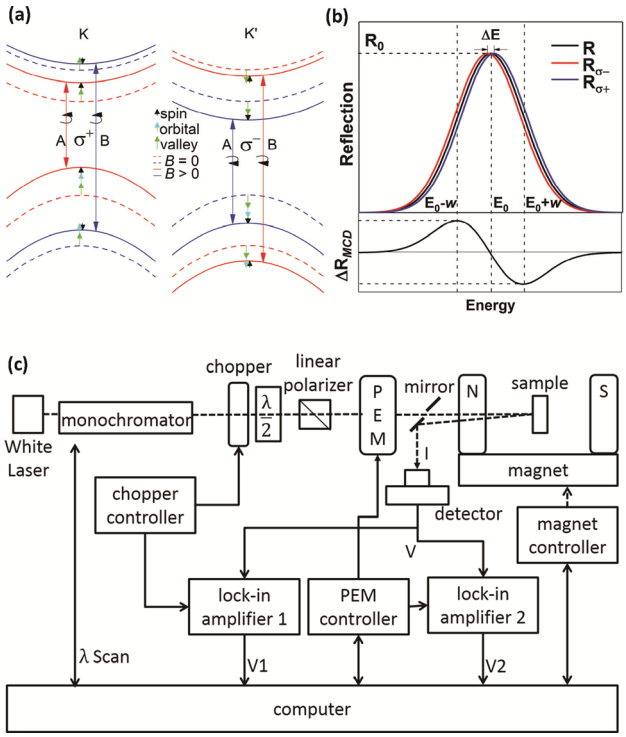

FIG. 1. (a) Schematic drawing of the conduction and valence bands (red curves for spin-up and blue curves for spin-down) in the K and K' valleys of monolayer MoS_2 at zero field (dashed curves) and non-zero field (solid curves), showing the valley-dependent optical selection rules for $\sigma+$ and $\sigma-$ light (bi-directional arrows) and the three contributions to the Zeeman shifts (black arrow for spin, cyan arrow for atomic orbital, and green arrow for valley). (b) Scheme of reflection MCD spectroscopy to probe the excitonic Zeeman splitting (assuming $\Delta E > 0$). The Gaussian lines in the top are reflection spectra, among which the black line is the original degenerate reflection spectrum of $\sigma-$ and $\sigma+$ light at zero field, the red line for $\sigma-$ light, and the blue line for $\sigma+$ light at non-zero field. The derivative-like line in the bottom is the difference between the reflection spectra of $\sigma-$ and $\sigma+$ light. For the sake of observation, some parameters are exaggerated to different extents. (c) Schematic diagram of the MCD experimental setup.

1(c). Both the reflection and MCD spectra could be obtained simultaneously with this system. MCD spectra peaks with a high signal-to-noise ratio are observed at the A and B exciton resonant energy levels under low magnetic fields. According to the field dependent MCD measurements, the valley Zeeman splitting and the corresponding effective g-factors of A and B excitons are extracted to be -3.83 ± 0.05 and -4.06 ± 0.07, respectively. We demonstrated that MCD spectroscopy is a very sensitive and feasible technique in the valleytronics studies of layered materials.

Monolayer MoS_2 samples were grown by chemical vapor deposition (CVD) inside a furnace equipped with a quartz tube.[20] Sapphire substrates were placed face-down above a crucible containing MoO_3 powder. This crucible was put downstream in a distance away from the center of the furnace, and another crucible with sulfur powder was placed at the upstream. The furnace was heated up to 850 °C with 60 sccm Ar flow at atmospheric pressure. After holding at 850 °C for 15 min, the furnace was cooled down naturally to room temperature. The wavelength tunable laser was obtained by using a super-continuum white light source equipped with a monochromator. The polarization of the monochromatic laser was modulated using the combination of a linear polarizer and a 50 kHz photoelastic modulator. To measure the reflectance intensity, the laser was also modulated with a 177 Hz chopper. The reflected light from the sample was detected using a Si photodetector. The reflectance and MCD signals were measured using a two lock-in amplifier with reference frequencies of 177 Hz and 50 kHz, respectively. The sample was placed inside a microscopic vacuum cryostat. A variable magnetic field along the incident direction of the excitation laser is provided by a superconducting magnet.

Transmission MCD spectroscopy has been employed in quantum dot solutions.[21–23] Here, we utilized the reflection setup instead of transmission because the reflectance is more suitable for materials on opaque substrates. The origin of MCD signals is the difference in the spectrum of left circularly polarized light and right circularly polarized light, as shown in Fig. 1(b). The excitonic transitions would introduce individual peaks on the reflectance spectrum.[24] In this way, it could be described as a Gaussian line centered at energy E_0,[15,25] $R(E) = R_0 \exp[-(E - E_0)^2/2w^2]$, where R_0 is the height of the reflection peak and $2w$ is the linewidth as defined. When a perpendicular magnetic field is applied, the excitonic transition is splitted into two components centered at $E_0 \pm \frac{1}{2}\Delta E$, where $\Delta E = g\mu_B B$ is the Zeeman splitting energy, and the effective g-factor results from the coupling of the orbital, spin, and valley moments. In most cases, ΔE is much smaller than the peak linewidth ($\Delta E < 0.1w$), and the rigid-shift approximation could be applied.[26] The reflection difference (MCD signal) of $\sigma-$ and $\sigma+$ light can be evaluated to be

$$\begin{aligned}\Delta R_{MCD}(E) &= R_{\sigma^-}(E) - R_{\sigma^+}(E) \\ &= R\left(E + \frac{1}{2}\Delta E\right) - R\left(E - \frac{1}{2}\Delta E\right) \cong \frac{dR(E)}{dE}\Delta E,\end{aligned} \tag{1}$$

i.e., the MCD feature can be approximately described as the first derivative of the corresponding reflection peak times the Zeeman splitting. As shown in the bottom of Fig. 1(b), the typical MCD feature of one transition contains a zero-crossing point at energy E_0, a positive peak, and a negative valley. The relative position of the peak and valley reflects the sign of the energy splitting. The peak amplitude of the MCD feature $\Delta R_{MCD-peak}$ can be figured out to be $\Delta R_{MCD-peak} = -\Delta R_{MCD-valley} \cong -\frac{1}{\sqrt{e}}\frac{R_0}{w}\Delta E$. That is, the MCD amplitude is proportional to the Zeeman splitting and inversely proportional to the peak linewidth. In this way, the narrow exciton peak width is an important advantage of monolayers for large MCD signals. For a perfect Gaussian reflectance profile, the MCD peak and valley are centrosymmetric to each other with the zero-crossing point acting as a symmetric center. In most realistic cases, the peak and valley of MCD spectra are not perfectly symmetrical, which results from the deviation of the original reflectance peak from the Gaussian line shape. Thus, we can deduce the energy splitting through MCD peak-to-valley amplitude, reflectivity, and the peak linewidth

$$\Delta E = -\sqrt{e}w\frac{\Delta R_{MCD-peak} - \Delta R_{MCD-valley}}{2R_0}. \tag{2}$$

As shown in the following, small energy splitting of monolayer MoS_2 can be measured through MCD spectra even at room temperature.

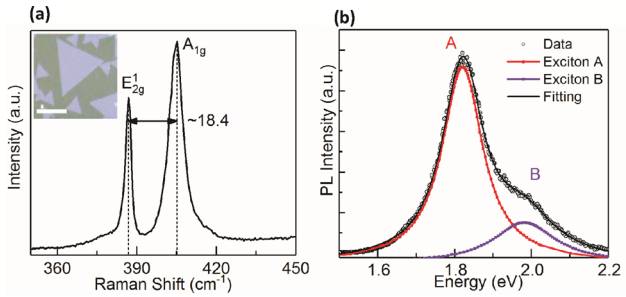

FIG. 2. (a) Room-temperature Raman spectrum of monolayer MoS_2 grown on sapphire substrates. The E^1_{2g} (~386.8 cm^{-1}) and A_{1g} (~405.2 cm^{-1}) peaks are two typical modes of monolayer MoS_2. The inset shows a representative optical microscope image of the MoS_2 sample. The scale bar is 10 μm. (b) PL spectrum of monolayer MoS_2. The red dashed curves are two Lorentzian function fits to the spectrum. The peak emissions at ~1.82 eV and ~1.98 eV correspond to A and B excitons, respectively. The excitation wavelength is 442 nm.

The quality of MoS_2 was investigated by Raman and PL spectroscopy. The measurements are performed with a Jobin-Yvon HR800 micro-Raman spectroscope at room temperature using a 442 nm excitation laser. As shown in Fig. 2(a), two characteristic Raman modes of MoS_2 are observed: E^1_{2g} (~386.8 cm^{-1}) and A_{1g} (~405.2 cm^{-1}), and the frequency difference of the E^1_{2g} and A_{1g} peaks is measured to be 18.4 cm^{-1}, implying that it is a monolayer MoS_2 sample.[27,28] Figure 2(b) shows the PL spectrum with Lorentzian fits, exhibiting two peaks at ~1.82 eV and ~1.98 eV, which correspond to A and B excitons, respectively. Both Raman and PL signals of our sample were in good agreement with previous literature,[29–32] indicating the fine monolayer nature and high quality of the sample.

The magnetic field dependent reflection spectra of monolayer MoS_2 are shown in Fig. 3(a). Two apparent peaks centered at 1.875 eV and 2.023 eV were observed, which were in good agreement with the transition energy of MoS_2 A and B excitons. This behavior shows that the room-temperature optical property of monolayer MoS_2 is dominated by the excitons because of their large binding energy.[7] The A and B excitons induced peaks superimposed on a relative flat background, and the reflectance spectrum can be well decomposed with two Gaussian lines (blue dashed line) with a smooth background (red dashed line), as shown in the inset of Fig. 3(a). With the analysis of the reflectance spectra, three important parameters can be extracted: the excitonic transition energies (E_0): ~1.875 eV for the A exciton and ~2.023 eV for the B exciton; the linewidth of each peak, $2w_A \cong 43$ meV and $2w_B \cong 68$ meV; and the height of each peak, $R_0^A \cong 0.0130$ and $R_0^B \cong 0.0137$. When the magnetic field was varied from −3 T to 3 T, the spectra resemble others and no obvious peak shift can be distinguished in accordance with the maxima of the spectra. This is because the valley Zeeman splitting induced peak shifts are much smaller than their linewidths, and the resolution of reflectance spectra is not high enough to extract the energy splitting under a low magnetic field.

Figure 3(b) shows the room-temperature MCD spectra of monolayer MoS_2 at different magnetic fields, and the MCD intensity is plotted as $\Delta R_{MCD}/R_0$, where R_0 is the height of the Gaussian lines as discussed above, which is

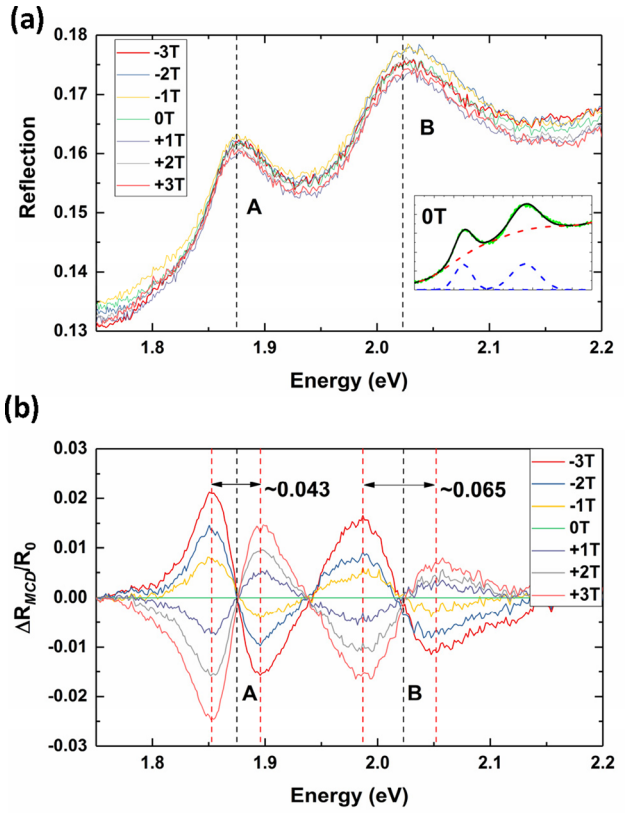

FIG. 3. (a) Room-temperature reflection spectra at different magnetic fields. The A and B exciton resonance peaks are clearly resolved. The inset shows the 0 T reflection spectrum, fitting to two Gaussian peaks (blue dashed curves) with a smooth background (red dashed curve). (b) Corresponding MCD spectra plotted as $\Delta R^X_{MCD}/R^X_0$ ($X = A, B$), where R^X_0 is extracted from (a). The original 0 T ΔR is taken as the systematic background, excluded by all the original ΔR at different fields.

extracted from the reflection spectra. Two typical MCD features as discussed before are observed at non-zero field. The two zero-crossing points of the MCD spectra are ~1.875 eV and ~2.023 eV, which are perfectly consistent with the exciton induced reflectance peaks A and B. Thus, we can assign these two features to be A and B, which originate from the A and B excitons respectively. It is worth noting that the exciton peaks of MCD spectra are deviated from being perfectly centrosymmetric as shown in Fig. 1(b), and the low energy side MCD magnitude is a little larger than the high energy side, which results from the fact that the excitonic transition rate of monolayer MoS_2 is not an ideal Gaussian profile at room temperature. Under a micro-perspective, the MCD originated from the transition possibility difference of left and right circular polarized photons. The transition possibility is determined by the Fermi's golden rule and is proportional to the transition matrix element and the transition allowed density of states, and both the band structure and the carrier occupation have influences on the spectrum.

Under a positive magnetic field, the MCD signal sign is negative at the low-energy side and positive at the high-energy side for both A and B-features, indicating that the effective g-factor of both excitonic transitions is negative. With the decreasing magnetic field from 3 T to 1 T, the amplitude of A and B features decreased proportionally, and the MCD spectrum is completely inverse when the magnetic field is reversed. This is in good agreement with our theory.

Furthermore, the MCD signal is proportional to the valley Zeeman splitting ΔE, which is proportional to the magnetic field. As shown in Figs. 3(a) and 3(b), the zero-crossing points are accurately consistent with the maximum of A and B exciton related peaks in the reflection spectra, suggesting that MCD spectroscopy can provide a precise determination of the excitonic transition energy. In addition, the energy difference of the MCD maximum and minimum is ~43 meV and ~65 meV for A and B-features, respectively, which are highly consistent with the linewidth of A and B exciton related peaks we extracted from the reflectance spectra and in perfect agreement with our theory. It is worth noting that MCD spectroscopy offers an alternative way to acquire the exciton linewidth accurately because it naturally eliminates the backgrounds that are irrelevant in the reflectance spectra.

Using the peak-to-valley value of the MCD feature and the linewidth, we extracted the valley Zeeman splitting of A and B excitons separately according to Eq. (2), and the results are shown in Fig. 4. The splitting of A exciton transition scales linearly with the applied magnetic field at a rate of -222 ± 3 μeV T^{-1}, corresponding to an effective g-factor of $g_A = -3.83\pm0.05$. The B exciton transition behaves similarly to the A exciton, and its splitting scales linearly with the applied magnetic field at a rate of -235 ± 4 μeV T^{-1}, corresponding to an effective g-factor of $g_B = -4.06\pm0.07$. Although the B exciton has a larger energy splitting coefficient than the A exciton, its MCD peak-to-valley value is smaller. The reason is that the B exciton exhibits a wider linewidth than the A exciton, which is a reflectance of its transition-allowed density of state distribution. Besides the phonon scattering induced broadening, temperature independent broadening mechanisms, such as impurities and dislocation scattering, also play an important role in the linewidth of exciton peaks. It has been demonstrated theoretically that the wider linewidth of the B exciton peak originates from the Dexter-like intervalley coupling.[33]

In a two-band tight-binding model where the effective mass is the same for both conduction and valence bands,[34] the valley magnetic moment does not affect the exciton splitting, and so, the atomic orbital magnetic moment solely works and contributes to a total exciton splitting of $-4\mu_B B$. In a more general picture, the effective mass is different for electrons and holes, and thus, the exciton valley splitting exhibits a little deviation away from $-4\mu_B B$.[12,14,15] The extracted g-factor values of A and B excitons agree well with the expectations of these models and those inferred from the polarization-resolved absorption spectra at magnetic fields up to 65 T.[14,15] The deviations away from $g = -4$ can be ascribed to the modification of valley orbital contribution. The manipulation of spin and valley is critical for existing and emerging quantum technologies, and the measurement and manipulation of the related effective g-factor can play an important role. Our results demonstrate that MCD is a feasible non-contact method to realize the manipulation of the valley and spin degrees of freedom in monolayer materials.

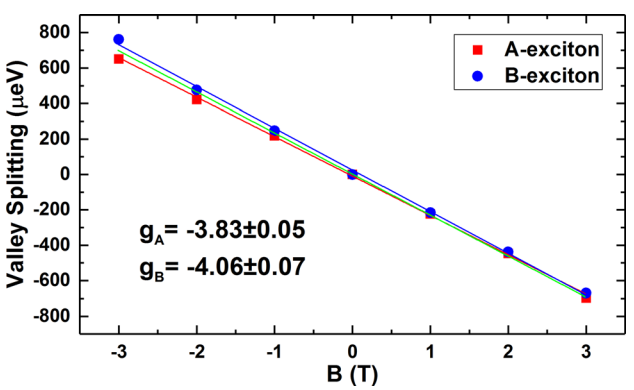

FIG. 4. The extracted valley Zeeman splitting versus magnetic field: red solid squares for the A exciton and blue solid circles for the B exciton. The red and blue lines are linear fits to extract effective g-factors for A and B excitons, respectively, while the green line corresponds to a splitting of $-4\mu_B$.

In summary, we studied the room-temperature reflection MCD spectra of monolayer MoS_2 on sapphire substrates. The MCD spectra exhibit obvious signals at the A and B excitonic transitions at room temperature even under a very low magnetic field. We obtained the room temperature valley Zeeman splitting to be -222 ± 3 μeV T^{-1} for the A exciton and -235 ± 4 μeV T^{-1} for the B exciton and derived the g-factors of monolayer MoS_2 on sapphire as -3.83 ± 0.05 for the A exciton and -4.06 ± 0.07 for the B exciton, respectively, which agreed well with the theoretical predictions. The MCD signals result from the magnetic perturbation (the Zeeman effect) of the states involved in optical transitions responsible for light-matter interactions. It can be used to study the influence of the external magnetic field on the electronic state of the sample, which is universal for all materials. Besides the original reflectance spectra, a new dimension (ΔR) is added, and the magnetic response of paramagnetic materials, as well as the magnetism properties of ferromagnetic materials, can be characterized accurately. Our work demonstrates that MCD spectroscopy can be a feasible method to study the valleytronics of monolayer MoS_2 and can be widely expanded to other 2D materials. It can also be further generalized to the magnetism related studies of low dimensional materials and heterostructures.

C. Shen and J. Zhang acknowledge the support from the NSFC Grant Nos. 11404324, 11574305, and 51527901. X. F. Liu acknowledges the support from the Open Project of Key Laboratory for UV-emitting Materials and Technology of Ministry of Education (No. 130028699), the National Natural Science Foundation of China (No. 21673054), and the Key Research Program of Frontier Science, CAS (No. QYZDB-SSW-SYS031).

[1]K. F. Mak, C. Lee, J. Hone, J. Shan, and T. F. Heinz, Phys. Rev. Lett. **105**(13), 136805 (2010).
[2]Q. H. Wang, K. Kalantar-Zadeh, A. Kis, J. N. Coleman, and M. S. Strano, Nat. Nano **7**(11), 699–712 (2012).
[3]R. Lv, J. A. Robinson, R. E. Schaak, D. Sun, Y. F. Sun, T. E. Mallouk, and M. Terrones, Acc. Chem. Res. **48**(1), 56–64 (2015).
[4]X. Ling, Y. X. Lin, Q. Ma, Z. Q. Wang, Y. Song, L. L. Yu, S. X. Huang, W. J. Fang, X. Zhang, A. L. Hsu, Y. Q. Bie, Y. H. Lee, Y. M. Zhu, L. J. Wu, J. Li, P. Jarillo-Herrero, M. Dresselhaus, T. Palacios, and J. Kong, Adv. Mater. **28**(12), 2322–2329 (2016).
[5]W. Xu, W. Liu, J. F. Schmidt, W. Zhao, X. Lu, T. Raab, C. Diederichs, W. Gao, D. V. Seletskiy, and Q. Xiong, Nature **541**(7635), 62–67 (2017).
[6]H. Zeng and X. Cui, Chem. Soc. Rev. **44**(9), 2629–2642 (2015).
[7]J. Xiao, M. Zhao, Y. Wang, and X. Zhang, Nanophotonics **6**(6), 1309–1328 (2017).

[8]H. P. Komsa and A. V. Krasheninnikov, Phys. Rev. B **86**(24), 241201 (2012).
[9]A. T. Hanbicki, M. Currie, G. Kioseoglou, A. L. Friedman, and B. T. Jonker, Solid State Commun. **203**, 16–20 (2015).
[10]A. F. Rigosi, H. M. Hill, K. T. Rim, G. W. Flynn, and T. F. Heinz, Phys. Rev. B **94**(7), 075440 (2016).
[11]S. Kim, K. Kim, J. U. Lee, and H. Cheong, 2D Mater. **4**(4), 045002 (2017).
[12]A. Srivastava, M. Sidler, A. V. Allain, D. S. Lembke, A. Kis, and A. Imamoglu, Nat. Phys. **11**(2), 141–147 (2015).
[13]D. MacNeill, C. Heikes, K. F. Mak, Z. Anderson, A. Kormanyos, V. Zolyomi, J. Park, and D. C. Ralph, Phys. Rev. Lett. **114**(3), 037401 (2015).
[14]A. V. Stier, K. M. McCreary, B. T. Jonker, J. Kono, and S. A. Crooker, Nat. Commun. **7**, 10643 (2016).
[15]A. A. Mitioglu, K. Galkowski, A. Surrente, L. Klopotowski, D. Dumcenco, A. Kis, D. K. Maude, and P. Plochocka, Phys. Rev. B **93**(16), 165412 (2016).
[16]G. B. Liu, W. Y. Shan, Y. G. Yao, W. Yao, and D. Xiao, Phys. Rev. B **88**(8), 085433 (2013).
[17]G. Aivazian, Z. R. Gong, A. M. Jones, R. L. Chu, J. Yan, D. G. Mandrus, C. W. Zhang, D. Cobden, W. Yao, and X. Xu, Nat. Phys. **11**(2), 148–152 (2015).
[18]C. Zhao, T. Norden, P. Y. Zhang, P. Q. Zhao, Y. C. Cheng, F. Sun, J. P. Parry, P. Taheri, J. Q. Wang, Y. H. Yang, T. Scrace, K. F. Kang, S. Yang, G. X. Miao, R. Sabirianov, G. Kioseoglou, W. Huang, A. Petrou, and H. Zeng, Nat. Nanotechnol. **12**(8), 757–762 (2017).
[19]C. Jiang, F. Liu, J. Cuadra, Z. Huang, K. Li, A. Rasmita, A. Srivastava, Z. Liu, and W. B. Gao, Nat. Commun. **8**(1), 802 (2017).
[20]D. Dumcenco, D. Ovchinnikov, K. Marinov, P. Lazić, M. Gibertini, N. Marzari, O. L. Sanchez, Y.-C. Kung, D. Krasnozhon, M.-W. Chen, S. Bertolazzi, P. Gillet, A. Fontcuberta i Morral, A. Radenovic, and A. Kis, Acs Nano **9**(4), 4611–4620 (2015).
[21]C. J. Barrows, V. A. Vlaskin, and D. R. Gamelin, J. Phys. Chem. Lett. **6**(15), 3076–3081 (2015).
[22]F. Muckel, J. Yang, S. Lorenz, W. Baek, H. Chang, T. Hyeon, G. Bacher, and R. Fainblat, Acs Nano **10**(7), 7135–7141 (2016).
[23]H. Yao and T. Shiratsu, J. Phys. Chem. C **121**(1), 761–768 (2017).
[24]H. L. Liu, C. C. Shen, S. H. Su, C. L. Hsu, M. Y. Li, and L. J. Li, Appl. Phys. Lett. **105**(20), 201905 (2014).
[25]N. Lundt, S. Klembt, E. Cherotchenko, S. Betzold, O. Iff, A. V. Nalitov, M. Klaas, C. P. Dietrich, A. V. Kavokin, S. Hofling, and C. Schneider, Nat. Commun. **7**, 13328 (2016).
[26]D. Steele, J. C. Whitehead, P. Meares, G. Doggett, R. Grice, and J. M. Hollas, J. Chem. Soc. Faraday Trans. 2 **80**, 1503–1506 (1984).
[27]X. Zhang, X. F. Qiao, W. Shi, J. B. Wu, D. S. Jiang, and P. H. Tan, Chem. Soc. Rev. **44**(9), 2757–2785 (2015).
[28]G. Kioseoglou, A. T. Hanbicki, M. Currie, A. L. Friedman, D. Gunlycke, and B. T. Jonker, Appl. Phys. Lett. **101**(22), 221907 (2012).
[29]X. Luo, Y. Y. Zhao, J. Zhang, M. Toh, C. Kloc, Q. H. Xiong, and S. Y. Quek, Phys. Rev. B **88**(19), 195313 (2013).
[30]Y. J. Zhan, Z. Liu, S. Najmaei, P. M. Ajayan, and J. Lou, Small **8**(7), 966–971 (2012).
[31]C. Lee, H. Yan, L. E. Brus, T. F. Heinz, J. Hone, and S. Ryu, Acs Nano **4**(5), 2695–2700 (2010).
[32]T. Korn, S. Heydrich, M. Hirmer, J. Schmutzler, and C. Schuller, Appl. Phys. Lett. **99**(10), 102109 (2011).
[33]I. Bernal-Villamil, G. Berghauser, M. Selig, I. Niehues, R. Schmidt, R. Schneider, P. Tonndorf, P. Erhart, S. M. de Vasconcellos, R. Bratschitsch, A. Knorr, and E. Malic, 2D Mater. **5**(2), 025011 (2018).
[34]X. D. Xu, W. Yao, D. Xiao, and T. F. Heinz, Nat. Phys. **10**(5), 343–350 (2014).